

A Diffusion Probabilistic Prior for Low-Dose CT Image Denoising

Xuan Liu¹, Yaoqin Xie², Songhui Diao², Shan Tan^{1*}, and Xiaokun Liang^{2**}

¹ School of Artificial Intelligence and Automation, Huazhong University of Science and Technology, Wuhan 430074, China

² Institute of Biomedical and Health Engineering, Shenzhen Institutes of Advanced Technology, Chinese Academy of Sciences, Shenzhen 518055, China
liuxuan99@hust.edu.cn

Abstract. Low-dose computed tomography (CT) image denoising is crucial in medical image computing. Recent years have been remarkable improvement in deep learning-based methods for this task. However, training deep denoising neural networks requires low-dose and normal-dose CT image pairs, which are difficult to obtain in the clinic settings. To address this challenge, we propose a novel fully unsupervised method for low-dose CT image denoising, which is based on denoising diffusion probabilistic model—a powerful generative model. First, we train an unconditional denoising diffusion probabilistic model capable of generating high-quality normal-dose CT images from random noise. Subsequently, the probabilistic priors of the pre-trained diffusion model are incorporated into a Maximum A Posteriori (MAP) estimation framework for iteratively solving the image denoising problem. Our method ensures the diffusion model produces high-quality normal-dose CT images while keeping the image content consistent with the input low-dose CT images. We evaluate our method on a widely used low-dose CT image denoising benchmark, and it outperforms several supervised low-dose CT image denoising methods in terms of both quantitative and visual performance.

Keywords: Low-dose CT · Diffusion model · Unsupervised learning.

1 Introduction

Low-dose computed tomography(CT) has attracted growing attention due to its significant reduction in radiation exposure [9]. However, the downside of low-dose CT is that it often produces poor-quality reconstructed images with non-negligible noise, which can potentially impede accurate diagnosis [14,26]. To address this issue, many algorithms have been developed to enhance the image quality of low-dose CT. These methods can be broadly categorized into sinogram filtering [1,15], iterative reconstruction [20,24], and image denoising [4,12]. Among these methods, low-dose CT image denoising is the most widely used as

* Shan Tan is corresponding author.

** Xiaokun Liang is corresponding author.

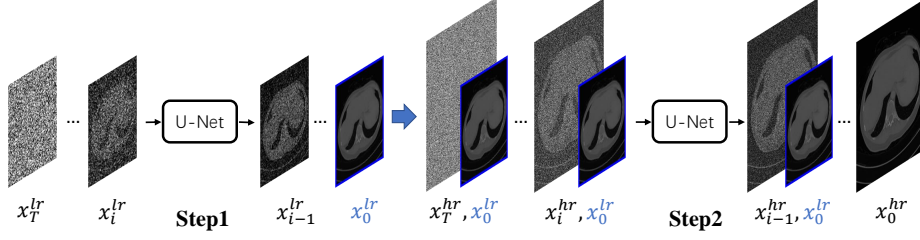


Fig. 1. The overall generation process of our pre-trained diffusion models. At the first step, a low-resolution CT image x_0^{lr} is generated from random noise x_T^{lr} . At the second step, the generated low-resolution CT images is input to a conditional diffusion model to generate a high-resolution CT image.

it does not involve the reconstruction process and can be applied to different CT imaging systems.

In the last decade, with the rapid development of deep learning techniques, deep neural networks have been widely used in low-dose CT image denoising and achieved significant success [4,9,27,28]. Typically, deep learning-based methods adopt a supervised learning framework, where the end-to-end mapping from low-dose to normal-dose CT images is learned from a large set of paired training data. However, the success of supervised deep learning algorithms hinges heavily on availability of large amounts of paired training data [13]. Unfortunately, it is challenging to acquire such data in the clinic due to the “as low as reasonably achievable” principle [2]. Therefore, it is essential to design novel methods that can effectively exploit the high performance of deep neural networks while minimizing the need for labeled data.

We propose a fully unsupervised method for denoising low-dose CT images using only normal-dose CT images for training. Unlike the supervised deep learning algorithms, our method utilizes neural networks to learn the prior of normal-dose CT images, rather than the mapping from low-dose to normal-dose CT images, which has been explored in recent studies [10,17,22].

To begin, we employ an unconditional denoising diffusion probabilistic model [7,8,18,21,23] (referred to as diffusion model hereafter) with normal-dose CT images for training. With the powerful generative ability of the diffusion model, we can generate realistic normal-dose CT images from random noise. Specifically, we first generate low-resolution images of size 128×128 from random noise and then produce high-resolution images by using the low-resolution images as conditions, as shown in Fig. 1.

However, the generation of diffusion models is inherently random, which pose a significant challenge for achieving low-dose CT image denoising without the aid of a supervised diffusion model [25]. To overcome this limitation, we design an algorithm that integrates an unconditional diffusion model into the denoising framework. Specifically, we incorporate low-dose CT images into each iteration of the diffusion model’s generation process, ensuring a favorable like-

likelihood match between the generated images and the input low-dose images. As a result, the diffusion model is able to produce high-quality counterpart of the input low-dose CT images, achieving effective low-dose CT image denoising.

The contributions of our proposed method are summarized as follows: (1) We successfully train an unconditional diffusion model on a large-scale CT image dataset, which is capable of generating realistic normal-dose CT images from random noise. To the best of our knowledge, this is the first time an unconditional diffusion model has been trained successfully on such a large-scale CT image dataset. (2) We propose an algorithm that incorporates the pre-trained diffusion model into the denoising framework. This algorithm enables fully unsupervised low-dose CT image denoising. (3) Our method demonstrates promising results in terms of both visual effects and indices, outperforming several supervised deep learning-based methods in low-dose CT image denoising.

2 Method

2.1 Normal-dose CT Image Generation with Diffusion Models

Given a set of data $x_0 \sim q(x_0)$, an unconditional diffusion model defines a fixed forward process $q(x_{0:T}) := q(x_0) \prod_{t=1}^T q(x_t | x_{t-1})$ with constant parameters $\{\bar{\alpha}_t\}_{t=1,\dots,T}$. The forward process is defined as a Markov chain where the probability distribution at each timestep is solely dependent on the distribution at the previous timestep. The forward process progressively adds noise to x_0 [21]. The reverse process $p_\theta(x_{0:T}) := p(x_T) \prod_{t=1}^T p_\theta(x_{t-1} | x_t)$ is defined as a Markov chain with learnable parameters θ . The training loss is derived by minimizing the variational bound of the negative log likelihood $-\log p_\theta(x_0)$ which is calculated by $q(x_{0:T})$ and $p_\theta(x_{0:T})$.

Given a dataset of image pairs (x_0, c) , a conditional diffusion model maintains the same forward process as an unconditional model, which is independent of conditional variable c . However, the reverse process $p_\theta(x_{0:T} | c)$ integrates c as an additional condition. Similarly, the training loss is derived by minimizing the variational bound of the negative log conditional distribution $-\log p_\theta(x_0 | c)$.

As shown in Fig. 1, we use a two-step cascade of diffusion models to generate normal-dose CT images. The first model is an unconditional diffusion model that generates low-resolution normal-dose CT images of size 128×128 from random noise. The second model is a conditional diffusion model that uses the low-resolution images generated in the first step as conditions to generate high-resolution normal-dose CT images of size 512×512 . The overall model is unconditional since it only uses normal-dose CT images without any accompanying labels for training.

2.2 Low-dose CT Image Denoising with Diffusion Prior

In this Section, we design an algorithm for image **D**enoising with **D**iffusion **p**rior, aka Dn-Dp. We will first describe the algorithm in a general case and then apply

it to the specific problem of low-dose CT image denoising using our pre-trained diffusion models.

Algorithms In image denoising problems, the corruption is always modeled as,

$$y_0 = x_0 + n. \quad (1)$$

The goal of this study is to estimate x_0 based on the given value of y_0 . To achieve this, we rely on a well-trained diffusion model that accurately captures the prior distribution of x_0 using forward process parameters $\{\bar{\alpha}_t\}_{t=1,\dots,T}$ and reverse process parameters θ . The aim is to use the diffusion prior to effectively denoise the y_0 . The concrete method is outlined below.

In diffusion models, x_t at timestep $t = 1, \dots, T$ can be generated from x_0 based on the forward process as,

$$x_t = \sqrt{\bar{\alpha}_t}x_0 + \sqrt{1 - \bar{\alpha}_t}\epsilon_t, \quad (2)$$

where $\epsilon_t \sim \mathcal{N}(0, I)$ is picked from the normal distribution. We generate $y_t(t = 1, \dots, T)$ from y_0 in the same way with the same ϵ_t ,

$$y_t = \sqrt{\bar{\alpha}_t}y_0 + \sqrt{1 - \bar{\alpha}_t}\epsilon_t. \quad (3)$$

By substituting Eq. (1) and Eq. (2) to Eq. (3), and setting $\bar{\alpha}_0 = 1$, the following equation is obtained for $t = 0, \dots, T$,

$$y_t = x_t + \sqrt{\bar{\alpha}_t}n. \quad (4)$$

Eq. (4) illustrates that there is a new denoising problem with noise $\sqrt{\bar{\alpha}_t}n$ at each timestep t . Because $\bar{\alpha}_t$ decreases as t increases and $\bar{\alpha}_T \approx 0$ [7], we can get $\hat{x}_T = y_T$ as an initialization. Then, for $t = T, \dots, 1$, diffusion priors $p_\theta(x_{t-1} | x_t)$ can be incorporated into a Maximum A Posteriori (MAP) framework [29] for the solution of x_{t-1} ,

$$\hat{x}_{t-1} = \arg \min_{x_{t-1}} [\|x_{t-1} - y_{t-1}\|^2 - \lambda_{t-1} \log p_\theta(x_{t-1} | \hat{x}_t)]. \quad (5)$$

In the reverse process of diffusion models, $p_\theta(x_{t-1} | \hat{x}_t)$ is a Gaussian distribution with mean $\mu_\theta(\hat{x}_t, t)$ and diagonal covariance matrix $\sigma_\theta^2(\hat{x}_t, t)I$. When $t > 1$, $\sigma_\theta > 0$ [7], so we have,

$$\hat{x}_{t-1} = \arg \min_{x_{t-1}} \left[\|x_{t-1} - y_{t-1}\|^2 + \frac{\lambda_{t-1}}{\sigma_\theta(\hat{x}_t, t)} \|x_{t-1} - \mu_\theta(\hat{x}_t, t)\|^2 \right], t > 1. \quad (6)$$

When $t = 1$, $\sigma_\theta = 0$, which means the final generation step of diffusion is deterministic,

$$\hat{x}_{t-1} = \mu_\theta(\hat{x}_t, t), \quad t = 1. \quad (7)$$

Algorithm 1 Image denoising with a pre-trained unconditional diffusion	Algorithm 2 Image denoising with a pre-trained conditional diffusion
Input: $y_0, \theta, \{\bar{\alpha}_t\}_{t=1,\dots,T}, \{\lambda_t\}_{t=1,\dots,T-1}$.	Input: $y_0, c, \theta, \{\bar{\alpha}_t\}_{t=1,\dots,T}, \{\lambda_t\}_{t=1,\dots,T-1}$.
Output: \hat{x}_0 .	Output: \hat{x}_0 .
1: Initialize $t = T$.	1: Initialize $t = T$.
2: Sample ϵ_T from $\mathcal{N}(0, I)$;	2: Sample ϵ_T from $\mathcal{N}(0, I)$;
3: $y_T = \sqrt{\bar{\alpha}_T}y_0 + \sqrt{1 - \bar{\alpha}_T}\epsilon_T$;	3: $y_T = \sqrt{\bar{\alpha}_T}y_0 + \sqrt{1 - \bar{\alpha}_T}\epsilon_T$;
4: $\hat{x}_T = y_T$.	4: $\hat{x}_T = y_T$.
5: while $t > 1$ do	5: while $t > 1$ do
6: Sample ϵ_t from $\mathcal{N}(0, I)$;	6: Sample ϵ_t from $\mathcal{N}(0, I)$;
7: $y_t = \sqrt{\bar{\alpha}_t}y_0 + \sqrt{1 - \bar{\alpha}_t}\epsilon_t$;	7: $y_t = \sqrt{\bar{\alpha}_t}y_0 + \sqrt{1 - \bar{\alpha}_t}\epsilon_t$;
8: Update \hat{x}_{t-1} according to Eq. (8);	8: Update \hat{x}_{t-1} according to Eq. (9);
9: $t = t - 1$;	9: $t = t - 1$;
10: end while	10: end while
11: $\hat{x}_0 = \mu_\theta(\hat{x}_1, 1)$.	11: $\hat{x}_0 = \mu_\theta(\hat{x}_1, 1, c)$.

Eq. (6) is a convex optimization problem, which has a closed-form solution. By solving Eq. (6) and combining Eq. (7), we can derive the solution of \hat{x}_{t-1} in each iteration as follows,

$$\hat{x}_{t-1} = \begin{cases} \left(y_{t-1} + \frac{\lambda_{t-1}}{\sigma_\theta(\hat{x}_t, t)} \mu_\theta(\hat{x}_t, t) \right) / \left(1 + \frac{\lambda_{t-1}}{\sigma_\theta(\hat{x}_t, t)} \right), & t > 1 \\ \mu_\theta(\hat{x}_t, t), & t = 1 \end{cases}. \quad (8)$$

Similarly, if the pre-trained diffusion model is conditional by c , the solution is,

$$\hat{x}_{t-1} = \begin{cases} \left(y_{t-1} + \frac{\lambda_{t-1}}{\sigma_\theta(\hat{x}_t, t, c)} \mu_\theta(\hat{x}_t, t, c) \right) / \left(1 + \frac{\lambda_{t-1}}{\sigma_\theta(\hat{x}_t, t, c)} \right), & t > 1 \\ \mu_\theta(\hat{x}_t, t, c), & t = 1 \end{cases}. \quad (9)$$

Eq. (8) and Eq. (9) illustrate the denoising process using a pre-trained unconditional or conditional diffusion model, in that y_{t-1} from Eq. (3) helps correct the diffusion model's outputs at each timestep, to ensure the accuracy of the finally generated images. The detailed algorithms are shown in Alg. 1 and Alg. 2

Given a low-dose CT image y_0^{hr} and two pre-trained diffusion models with parameters $\{\theta^{lr}, \{\bar{\alpha}_t^{lr}\}_{t=1,\dots,T}\}$ and $\{\theta^{hr}, \{\bar{\alpha}_t^{hr}\}_{t=1,\dots,T}\}$, we first obtain the low-resolution low-dose CT image y_0^{lr} by $4\times$ downsampling. Next, we input $y_0^{lr}, \theta^{lr}, \{\bar{\alpha}_t^{lr}\}_{t=1,\dots,T}, \{\lambda_t^{lr}\}_{t=1,\dots,T-1}$ into Alg. 1 to obtain the denoised low-resolution CT image \hat{x}_0^{lr} . Then, we input $y_0^{hr}, \hat{x}_0^{lr}, \theta^{hr}, \{\bar{\alpha}_t^{hr}\}_{t=1,\dots,T}, \{\lambda_t^{hr}\}_{t=1,\dots,T-1}$, where \hat{x}_0^{lr} is the condition, into Alg. 2 to obtain the high-resolution denoised CT image \hat{x}_0^{hr} . The overall workflow of our low-dose CT denoising method is shown in Fig. 2. In addition, we calculate the average of multiple denoising results for better performance [11] and accelerate the iterations following DDIM [21].

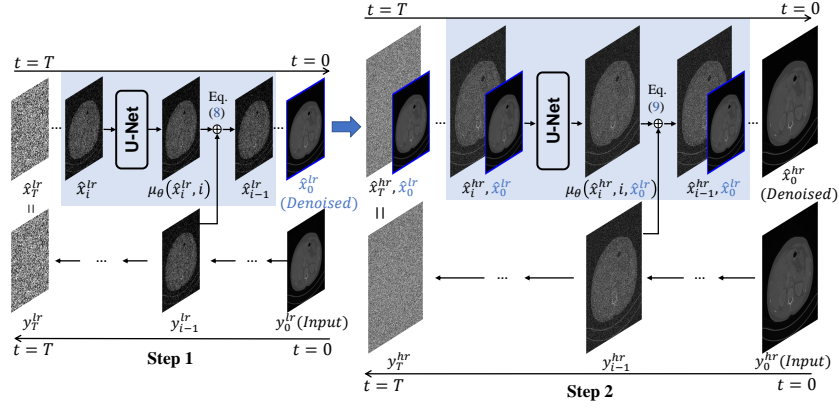


Fig. 2. The proposed low-dose CT image denoising workflow. At the first step, the low-resolution image y_0^{lr} is denoised and input to Step 2 as a condition. At the second step, high-resolution image y_0^{hr} is denoised.

Adaptive Strategy for λ In Alg. 1 and Alg. 2, $\{\lambda_t\}_{t=1,\dots,T-1}$ are hyper-parameters to trade off likelihood and prior. Empirically, lower noise level requires smaller λ . According to Eq. (4), the noise is $\sqrt{\bar{\alpha}_t}n$ at timestep t , where $\bar{\alpha}_t$ decreases from 1 to nearly 0 as t increases from 0 to T . Therefore, we tentatively set $\lambda_t = coef \cdot \sqrt{\bar{\alpha}_t}$.

However, different low-dose CT slices always exhibit varying noise levels, which results in a fixed *coef* cannot achieve the best denoising result for each low-dose CT image. We propose to select appropriate λ by estimating the noise level of each single input image. Specifically, we set a timestep t_λ . When $t > t_\lambda$, we estimate the noise level by the average pixel value $\mathcal{M}(y_0)$ of the input low-dose CT image y_0 . When $t \leq t_\lambda$, the diffusion model can roughly predict a clean CT image x_t^{pred} [21], we calculate the noise level by the variance of the estimated noise ($y_0 - x_t^{pred}$). We simply assume the coefficient of λ_t to be linearly related to the variance. As a result, we propose an adaptive strategy for λ as follows,

$$\lambda_t^{adap} = \begin{cases} \mathcal{M}(y_0) \cdot \lambda_0 \cdot \sqrt{\bar{\alpha}_t}, & t > t_\lambda \\ \left(a \cdot Var(y_0 - x_t^{pred}) + b \right) \cdot \sqrt{\bar{\alpha}_t}, & t \leq t_\lambda \end{cases}, \quad (10)$$

3 Experiments

3.1 Normal-dose CT Image Generation

We have trained the cascaded diffusion models on abdomen CT images obtained from low-dose CT and projection data (LDCT-PD) [5,16]. In Fig. 3, We display samples generated by our pre-trained diffusion models. To the best of our knowledge, this is the first unconditional diffusion model trained on a large-scale

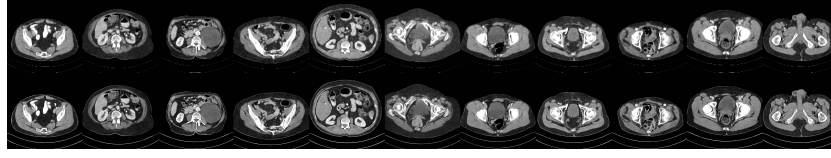


Fig. 3. Normal-dose CT images generated from random noise with our pre-trained diffusion models. The first row are the 128×128 low-resolution images. The second row are the corresponding 512×512 high-resolution images. The display window is $[-160, 240]$ HU.

Table 1. Denoising results with different λ on 80 CT images

	$\lambda_t^{cons} = coef \cdot \sqrt{\alpha_t}$					λ_t^{adap}
<i>coef</i>	0.002	0.003	0.004	0.005	0.006	
PSNR	26.32	26.67	26.82	26.85	26.83	26.88
SSIM	0.826	0.830	0.829	0.827	0.827	0.830

CT image dataset capable of generating high-resolution normal-dose CT images that are visually realistic and accurate. The pre-trained models will be released.

3.2 Study of λ

We evaluate our proposed adaptive strategy for λ on 80 low-dose CT images of 4 patients from the 2016 Low-dose CT Grand Challenge [4]. $\lambda_t^{cons} = coef \cdot \sqrt{\alpha_t}$ with constant coefficients are used for comparisons. Table 1 shows the denoising performance with different λ , which demonstrates our proposed adaptive λ achieves the best results. In Fig. 4, we show the denoised results of 2 different CT slices from one patient. The ROIs denoised with different λ are displayed as well as their corresponding PSNRs. As one can see, the two slices achieve the best denoising results with totally different λ . However, the proposed adaptive λ achieves promising denoising results for both slices.

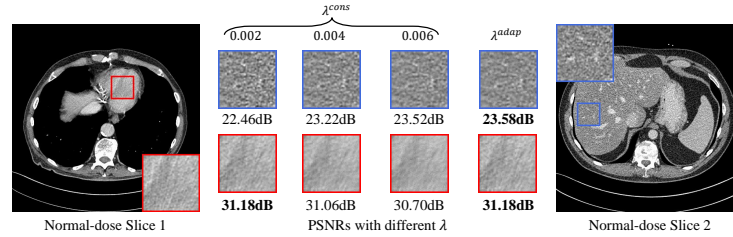
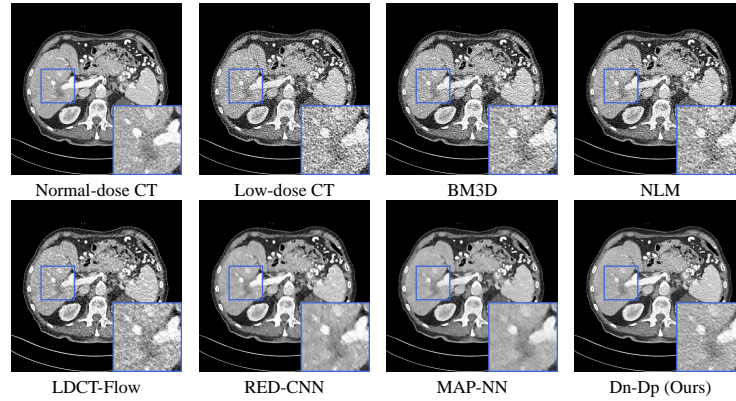


Fig. 4. Two slices favor totally different λ , while our proposed adaptive λ satisfies both of them. The display window is $[-160, 240]$ HU.

Table 2. Quantitative results on 1400 CT images of 4 patients.

Methods	Low-dose	BM3D	NLM	LDCT-Flow	RED-CNN	MAP-NN	Dn-Dp(Ours)
PSNR	22.60	25.15	24.97	25.24	27.26	27.28	27.31
SSIM	0.766	0.801	0.801	0.805	0.815	0.817	0.829

**Fig. 5.** Visual comparison of one CT image. The display window is $[-160, 240]$ HU.

3.3 Low-dose CT Image Denoising Results

We evaluate the effectiveness of our denoising method on a widely used dataset obtained from the 2016 Low-dose CT Grand Challenge. Specifically, we conduct tests on 1400 low-dose CT images from four patients, and we compare our methods against other denoising method, including two classic denoising methods, BM3D [6], NLM [3], an unsupervised method using unpaired training data, LDCT-Flow [13], and two famous supervised deep learning-based methods: RED-CNN [4] and MAP-NN [19]. The results are presented in Table 2, which shows that our method achieves the best quantitative results, as measured by PSNR and SSIM. It is noteworthy that our method achieves a higher PSNR than the supervised deep learning-based methods, even though MSE-based supervised training typically favors higher PSNR. Fig. 5 displays the denoising results of one CT image from test data. In this regard, BM3D and NLM fail to remove the low-dose CT noise, and the denoising results of RED-CNN and MAP-NN are obviously over-smoothed when compared to the realistic normal-dose CT image. This over-smoothing could potentially impede the subsequent diagnosis process. Although LDCT-Flow has a more realistic visual effect, it does not achieve the performance of our method. By leveraging the strong generative prior of diffusion models, our method achieves the best visual performance among the comparison methods.

4 Conclusion

In this paper, we introduce a denoising algorithm for low-dose CT that leverages the diffusion prior. We commence by training a cascaded diffusion model that can generate a low-resolution and high-resolution normal-dose CT image in a sequentially manner. Our denoising algorithm involves the iterative solution of multiple optimization problems, ensuring that the pre-trained diffusion model produces a high-quality image that is consistent with the input low-dose CT image. Our future research efforts will focus on integrating the diffusion prior into CT reconstruction to exploit the projection domain information more effectively.

References

1. Balda, M., Hornegger, J., Heismann, B.: Ray contribution masks for structure adaptive sinogram filtering. *IEEE transactions on medical imaging* **31**(6), 1228–1239 (2012)
2. Brenner, D.J., Hall, E.J.: Computed tomography—an increasing source of radiation exposure. *New England journal of medicine* **357**(22), 2277–2284 (2007)
3. Buades, A., Coll, B., Morel, J.M.: A non-local algorithm for image denoising. In: 2005 IEEE Computer Society Conference on Computer Vision and Pattern Recognition (CVPR’05). vol. 2, pp. 60–65. IEEE (2005)
4. Chen, H., Zhang, Y., Kalra, M.K., Lin, F., Chen, Y., Liao, P., Zhou, J., Wang, G.: Low-dose ct with a residual encoder-decoder convolutional neural network. *IEEE transactions on medical imaging* **36**(12), 2524–2535 (2017)
5. Clark, K., Vendt, B., Smith, K., Freymann, J., Kirby, J., Koppel, P., Moore, S., Phillips, S., Maffitt, D., Pringle, M., et al.: The cancer imaging archive (tcia): maintaining and operating a public information repository. *Journal of digital imaging* **26**(6), 1045–1057 (2013)
6. Dabov, K., Foi, A., Katkovnik, V., Egiazarian, K.: Image denoising by sparse 3-d transform-domain collaborative filtering. *IEEE Transactions on image processing* **16**(8), 2080–2095 (2007)
7. Ho, J., Jain, A., Abbeel, P.: Denoising diffusion probabilistic models. *Advances in Neural Information Processing Systems* **33**, 6840–6851 (2020)
8. Ho, J., Saharia, C., Chan, W., Fleet, D.J., Norouzi, M., Salimans, T.: Cascaded diffusion models for high fidelity image generation. *J. Mach. Learn. Res.* **23**(47), 1–33 (2022)
9. Jin, K.H., McCann, M.T., Froustey, E., Unser, M.: Deep convolutional neural network for inverse problems in imaging. *IEEE Transactions on Image Processing* **26**(9), 4509–4522 (2017)
10. Kavar, B., Elad, M., Ermon, S., Song, J.: Denoising diffusion restoration models. In: *Advances in Neural Information Processing Systems* (2022)
11. Kavar, B., Vaksman, G., Elad, M.: Snips: Solving noisy inverse problems stochastically. *Advances in Neural Information Processing Systems* **34**, 21757–21769 (2021)
12. Li, Z., Yu, L., Trzasko, J.D., Lake, D.S., Blezek, D.J., Fletcher, J.G., McCollough, C.H., Manduca, A.: Adaptive nonlocal means filtering based on local noise level for ct denoising. *Medical physics* **41**(1), 011908 (2014)
13. Liu, X., Liang, X., Deng, L., Tan, S., Xie, Y.: Learning low-dose ct degradation from unpaired data with flow-based model. *Medical Physics* **49**(12), 7516–7530 (2022)

14. Ma, J., Liang, Z., Fan, Y., Liu, Y., Huang, J., Chen, W., Lu, H.: Variance analysis of x-ray ct sinograms in the presence of electronic noise background. *Medical physics* **39**(7Part1), 4051–4065 (2012)
15. Manduca, A., Yu, L., Trzasko, J.D., Khaylova, N., Kofler, J.M., McCollough, C.M., Fletcher, J.G.: Projection space denoising with bilateral filtering and ct noise modeling for dose reduction in ct. *Medical physics* **36**(11), 4911–4919 (2009)
16. McCollough, C., Chen, B., Holmes, D., Duan, X., Yu, Z., Xu, L., Leng, S., Fletcher, J.: Low dose ct image and projection data [data set]. The Cancer Imaging Archive (2020)
17. Peng, C., Guo, P., Zhou, S.K., Patel, V.M., Chellappa, R.: Towards performant and reliable undersampled mr reconstruction via diffusion model sampling. In: *Medical Image Computing and Computer Assisted Intervention–MICCAI 2022: 25th International Conference, Singapore, September 18–22, 2022, Proceedings, Part VI*. pp. 623–633. Springer (2022)
18. Saharia, C., Ho, J., Chan, W., Salimans, T., Fleet, D.J., Norouzi, M.: Image super-resolution via iterative refinement. *IEEE Transactions on Pattern Analysis and Machine Intelligence* (2022)
19. Shan, H., Padole, A., Homayounieh, F., Kruger, U., Khera, R.D., Nitiwarangkul, C., Kalra, M.K., Wang, G.: Competitive performance of a modularized deep neural network compared to commercial algorithms for low-dose ct image reconstruction. *Nature Machine Intelligence* **1**(6), 269–276 (2019)
20. Sidky, E.Y., Pan, X.: Image reconstruction in circular cone-beam computed tomography by constrained, total-variation minimization. *Physics in Medicine & Biology* **53**(17), 4777 (2008)
21. Song, J., Meng, C., Ermon, S.: Denoising diffusion implicit models. *arXiv preprint arXiv:2010.02502* (2020)
22. Song, Y., Shen, L., Xing, L., Ermon, S.: Solving inverse problems in medical imaging with score-based generative models. In: *International Conference on Learning Representations* (2022), <https://openreview.net/forum?id=vaRCHVj0uGI>
23. Song, Y., Sohl-Dickstein, J., Kingma, D.P., Kumar, A., Ermon, S., Poole, B.: Score-based generative modeling through stochastic differential equations. In: *International Conference on Learning Representations* (2021), <https://openreview.net/forum?id=PXTIG12RRHS>
24. Sun, T., Sun, N., Wang, J., Tan, S.: Iterative cbct reconstruction using hessian penalty. *Physics in Medicine & Biology* **60**(5), 1965 (2015)
25. Xia, W., Lyu, Q., Wang, G.: Low-dose ct using denoising diffusion probabilistic model for $20\times$ speedup. *arXiv preprint arXiv:2209.15136* (2022)
26. Xu, J., Tsui, B.M.: Electronic noise modeling in statistical iterative reconstruction. *IEEE Transactions on Image Processing* **18**(6), 1228–1238 (2009)
27. Yang, Q., Yan, P., Zhang, Y., Yu, H., Shi, Y., Mou, X., Kalra, M.K., Zhang, Y., Sun, L., Wang, G.: Low-dose ct image denoising using a generative adversarial network with wasserstein distance and perceptual loss. *IEEE transactions on medical imaging* **37**(6), 1348–1357 (2018)
28. Zhang, Z., Yu, L., Liang, X., Zhao, W., Xing, L.: Transct: Dual-path transformer for low dose computed tomography. In: *International Conference on Medical Image Computing and Computer-Assisted Intervention*. Springer (2021)
29. Zoran, D., Weiss, Y.: From learning models of natural image patches to whole image restoration. In: *2011 international conference on computer vision*. pp. 479–486. IEEE (2011)